Journal of Colloid and Interface Science 578 (2020) 164–170

Contents lists available at ScienceDirect

Journal of Colloid and Interface Science

journal homepage: www.elsevier.com/locate/jcis

# Construction of an ultrasensitive electrochemical sensing platform for microRNA-21 based on interface impedance spectroscopy

Tianjiao Meng, Dan Zhao, Huimin Ye, Yue Feng, Huan Wang, Yufan Zhang *

*Key Laboratory of Medicinal Chemistry and Molecular Diagnosis of the Ministry of Education, Key Laboratory of Analytical Science and Technology of Hebei Province, College of Chemistry and Environmental Science, Hebei University, 071002 Baoding, PR China*

## HIGHLIGHTS

- An electrochemical sensing platform is constructed for detecting miR-21 based on interface impedance spectroscopy.
- The biosensor shows low limit of detection and wide dynamic correlation of miR-21.
- The proposed method is enzyme-free and PCR-free strategy.

## GRAPHICAL ABSTRACT

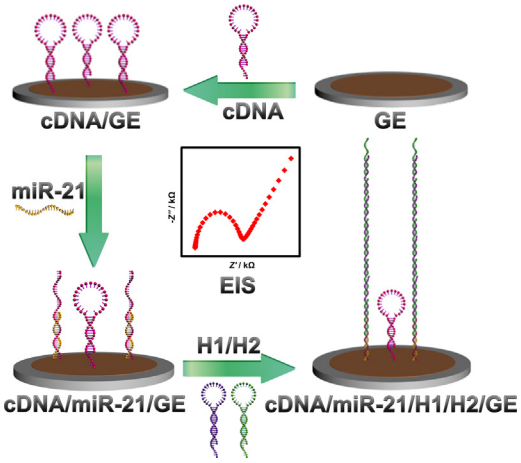


## ARTICLE INFO

*Article history:*
Received 22 January 2020
Revised 29 May 2020
Accepted 30 May 2020
Available online 1 June 2020

*Keywords:*
MicroRNA-21
Electrochemical impedimetric biosensor
Ultrasensitive electrochemical detection

## ABSTRACT

A hybridization chain reaction (HCR) amplification-based electrochemical impedimetric biosensor is fabricated for the quick, sensitive, and specific detection of miRNA-21 (miR-21) via monitoring of electrode interfacial property changes in real-time. Two sequences of H1 and H2 are adopted to trigger HCR amplification. A large amount of linear DNA concatemer are formed which could change the interfacial properties of the electrode. Interfacial charge transfer resistance difference ($R_{ct}$) is probed via electrochemical impedance spectroscopy (EIS) and Randles equivalent circuit. After amplifying via HCR, oligonucleotides with negatively charged repelling $[Fe(CN)_6]^{3-/4-}$ ions can form a spatial blockage. HCR amplification strategy markedly enhanced the electrochemical signal with a limit of detection (LOD) down to 4.63 fM (S/N = 3). This strategy exhibited excellent selectivity for three different miRNAs: miR-199a, miR-141, and miR-155. Moreover, results show that the proposed method can be applied to miR-21 detection in the total RNA extracted from five cells. This work presents an enzyme-free and label-free EIS nucleic acid sensor for sensitively and selectively detecting miR-21, offering a promising approach in early diseases diagnosis.



* Corresponding author.
*E-mail address:* zyf@hbu.edu.cn (Y. Zhang).

https://doi.org/10.1016/j.jcis.2020.05.118
0021-9797/

## 1. Introduction

Electrochemical biosensors have been widely utilized in energy resources, the life sciences, and other fields because of their simplicity of operation, quick responsiveness, inherent sensitivity, and good selectivity [1–4]. Currently, electrochemical biosensors have been efficiently applied in the detection of various miRNAs [5,6]. Among different electrochemical methods, electrochemical impedance spectroscopy (EIS) is an efficient method for investigating electrode surface change through the sinusoidal electric potential application with a variable frequency [7,8]. Utilizing equivalent circuits allows the experimental spectra to be fitted with the theoretical curve that corresponds to the selected circuit model, thereby obtaining the resistance values [9]. However, EIS-based label-free biosensors possess lower sensitivity than those with labeling methods. Therefore, nanomaterials and various amplification strategies have been utilized to enhance impedimetric sensing sensitivity [7]. Although most developed methodologies that relying various labels offer enhanced sensor sensitivity, they also increase the assay procedure complexity, time, and cost [10]. Moreover, the EIS can be seen as a label-free electrochemical method which can achieve transduction in the absence of labeled species. EIS have successfully been utilized to detect various biomolecules, such as toxins, bacteria, different kinds of DNA, and miRNAs during the last few years due to steric hindrance and electrostatic repulsion. For example, Miranda-Castro et al. constructed an impedimetric sensor to detect sensitively the uropathogenic E. coli cells by utilizing artificial recognition sites [11]. Azzouzi et al. successfully fabricated an integrated dual-functional recognition/amplification biosensor for the sensitive detection of microRNA-21 (miR-21) via EIS [12]. Kannan et al. constructed a cobalt oxide porous nanocubes-based impedimetric biosensor for the sensitive detection of hepatitis B virus DNA [13].

MicroRNA (miRNAs) is an endogenous, noncoding, single-stranded RNAs with approximately 18–24 nucleotides [14]. They are closely related to almost every cellular process, including post-transcriptional gene regulation, cell proliferation, differentiation, and apoptosis [15–18]. Sufficient evidence suggestes that miRNAs can emerge as significant diagnostic markers due to miRNAs over-expression in the cellular process [19–22]. Among them, miR-21 is over-expressed in multiple malignant tumors, including lung cancer, breast cancer, uterine cancer, gastric cancer, pancreatic cancer, liver cancer, cholangiocarcinoma, colon cancer, and prostate cancer, as well as participating in tumor occurrence and development through complex regulation [23–25]. Furthermore, the miR-21 content derived from five different cancer cells including breast (MCF-7), cervical (HeLa), non-small cell lung (A549), mouse leukemia cells of monocyte-macrophage (RAW 264.7), and human umbilical vein endothelial (HUVEC) was investigated to analyze the feasibility of the proposed impedimetric biosensor. Among these, HUVEC was utilized as an endogenous reference gene for normalization purposes. Therefore, accurate and sensitive miR-21 detection can be a powerful tool for clinical diagnosis and therapy.

Recently, many target amplification assays were explored to achieve highly sensitive miR-21 electrochemical determinations. The most common methods for achieving the target amplification are as follows: loop-mediated isothermal amplification (LAMP) [26], catalytic hairpin assembly (CHA) [27,28], strand-displacement amplification (SDA) [29], isothermal exponential amplification reaction (EXPAR) [30], and hybridization chain reaction (HCR) [31–34]. In a typical HCR, the initiator triggers a self-assembly reaction of two hairpins with partial complementarities to form alternate nucleic acids concatemers. HCR amplification strategies have proven to be a particularly effective method for fabricating the electrochemical nucleic acid biosensor because of its isothermal, enzyme-free, high amplification efficiency, and mild reaction conditions. For example, Zhou et al. constructed a novel electrochemical assay for sensitively detecting of miRNAs via non-linear HCR [35]. From Zhang's report, HCR amplification strategy and $MoS_2$-loaded G-quadruplex molecular beacon probes were utilized to improve sensitive detection of miRNA-199a/b-3p and miR-21 [36]. Cheng et al. successfully constructed mesoporous silica container biosensors for detecting miR-21 via CHA/HCR [5]. Also, Li et al. have constructed a biosensor for sensitively detecting miRNA-141 via a one-step introduction of a target-triggered branched HCR circuit [37].

In this paper, an electrochemical nucleic acid biosensing approach for miR-21 detection is proposed based on HCR strategy signal amplification coupled with EIS (Scheme 1). The thiol-functionalized capture hairpins (cDNA) were immobilized on the gold electrode (GE) surface. When the target miR-21 was presented in the system, the cDNA hairpin structures were opened. Thereafter, the released cDNA sequences are utilized to initiate the HCR reaction between two hairpin probes (H1 and H2), and many linear DNA concatemers can eventually be formed. The steric hindrance and electrostatic repulsion between the inherent negatives were induced via linear DNA concatemers, leading to a great increase of the interfacial electron transfer resistance ($R_{ct}$). The impedimetric biosensor also achieved miR-21 detection in human serum. The impedimetric biosensor combining the HCR signal amplification and EIS method obtained a wide linear range, high sensitivity, and excellent specificity toward miR-21.

## 2. Experimental

### 2.1. Reagent and apparatus

Gelred and loading buffer were received from Sangon, Inc. (Shanghai, China). Ethylenediaminetetraacetic acid disodium salt (EDTA), trichloromethane ($CHCl_3$), HCl, orthoboric acid 6-Mercapto-1-hexanol (MCH), and isopropanol were provided by MACKLIN Reagent Co. Ltd. *N*-hydroxysuccinimide (NHS, 98%), N-(3-dimethylaminopropyl)-*N*-ethylcarbodiimidehydrochloride (EDC, 98%), ammonium persulphate (APS), and tris were provided

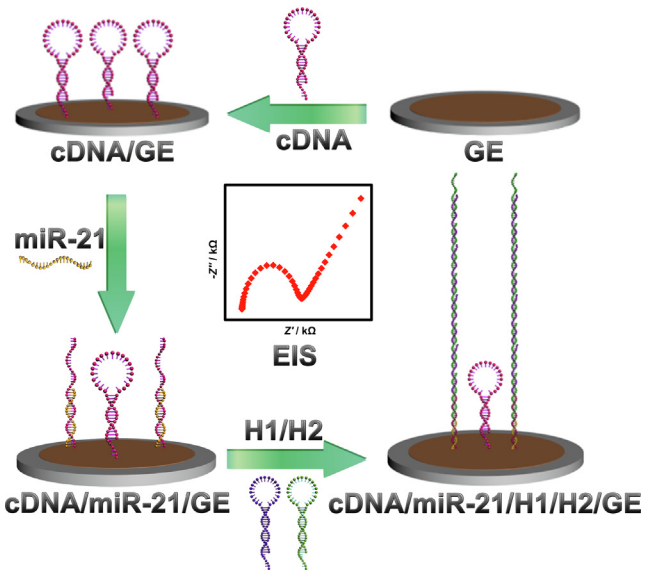


**Scheme 1.** A principle of impedimetric biosensing platform for detecting miR-21 based on HCR.

by Aladdin, Inc. (Shanghai, China). Diethyl pyrocarbonate (DEPC) and acrylamide were provided by Biosharp, Inc. (Hefei, China). *N,N,N′,N′*-Tetramethylethylenediamine (TEMED) was provided by Sigma-Aldrich, Inc. (Beijing, China). All HPLC purified oligonucleotides were provided by Sangon, Inc. (Shanghai, China) (Table 1). All electrochemical measurements were carried out with an AUTOLAB Electrochemical Workstation (Metrohm Instruments, Switzerland).

### 2.2. Extraction of total RNA in cells

The proposed method was investigated to detect the miR-21 content in total RNA, which were extracted from A549, HeLa, MCF-7, RAW 264.7, and HUVEC. In a typical trizol method, trizol can maintain RNA integrity during sample splitting or homogenization. The solution is divided into a water phase and an organic phase after chloroform is added. RNA is present in the aqueous phase, then, after taking out the aqueous phase, isopropanol can be utilized to precipitate and recover RNA. The trizol method has a high extraction efficiency. Also, the extracted total RNA can effectively avoid pollution by DNA and protein. Therefore, the trizol method has little influence on extracting RNA from cells. About $1 \times 10^6$ cells were rinsed by 0.1 M of PBS (pH 7.4) then dispersed in a non-enzymatic centrifuge tube containing 1 mL of trizol. Next, 200 μL of $CHCl_3$ was added into the non-enzymatic centrifuge tube to separate RNA. Then, the supernatant was carefully transferred into a fresh non-enzymatic centrifuge tube and washed with isopropanol and ethanol. Finally, total RNA was dispersed in 15 μL of DEPC then stored at −80 °C before utilization.

### 2.3. Preparation of the target-triggered amplification electrochemical biosensor

The GE was initially polished carefully with 0.3 and 0.05 μm of alumina powder on a polishing cloth of chamois leather, then it was sonicated in deionized water and ethanol for 30 s. Before the experiment, the DNA hairpin probes including cDNA, H1, and H2 were denatured at 95 °C for 5 min then gradually gradient cooled to room temperature to form a stem-loop structure before utilization. To reduce disulfide bonds, thiol-modified cDNA was dispersed in a TE buffer containing 10 mM TCEP for 1 h at room temperature. Then, 8 μL of cDNA (2.5 μM) was incubated on the well-cleaned GE surface at 4 °C for 14 h through the Au-S bond. Next, the prepared electrode was thoroughly washed with deionized water to remove physically adsorbed cDNA. Then, 10 μL of 1.0 mM MCH was dropped onto the modified electrode for 40 min to prevent nonspecific adsorption. Meanwhile, steric hindrance was minimized to enhance the modified electrode charge transfer. After rinsing with deionized water, 8 μL of target miR-21 was dropped onto the prepared electrode and incubated for 60 min at 37 °C. The mixed solution was prepared by mixing 8 μL of 2.5 μM H1 and 8 μL of 2.5 μM H2. Subsequently, the mixed solution was introduced to the prepared electrode for 80 min at 37 °C to trigger the HCR process, thereby producing numerous linear DNA concatamers. In the end, the self-assembly electrode was rinsed with deionized water then dried in nitrogen gas and stored in the air before utilization.

**Table 1**
The sequences of all oligonucleotides.

| Name | Sequence (5′–3′) |
|---|---|
| cDNA | SH-$(CH_2)_6$-TCAACATCAGTCTGATAAGCTA GCATCCTAGCTTATCAGACTGAAGCTA |
| H1 | TATCAGACTGAAGCTATTCAAAGT TAGCTTCAGTCTGATAA GCTAGGA |
| H2 | ACTTTGAATAGCTTCAGTCTGATATCCTAGCT TATCAGACTGAAGCTATT |
| miR-21 | UAGCUUAUCAGACUGAUGUUGA |
| miR-155 | UUAAUGCUAAUCGUGAUAGGGGU |
| miR-141 | UAACACUGUCUGGUAAAGAUGG |
| miR-199a | ACAGUAGUCUGCACAUUGGUUA |

### 2.4. Native polyacrylamide gel electrophoresis (PAGE)

Fifteen percent native polyacrylamide gel (5 mL of 30% acrylamide-bisacrylamide, 2.4 mL of deionized water, 2.5 mL of 5 × TBE, 100 μL of 10% APS, and 4 mL of TEMED) was utilized to characterize the the HCR process. The samples were dropped into each lane, then electrophoresis was run in 1 × TBE buffer operated at 100 V. Next, the gel was dyed with gelred for 30 min. Finally, the gel was scanned via a Bio-Red Imaging System.

## 3. Results and discussion

### 3.1. Analysis of the HCR via PAGE

HCR assembly process feasibility has been investigated by PAGE (Fig. S1). Lanes 1–4 were loaded with 5 μM of cDNA, 5 μM of H1, 5 μM of H2, and 20 μM of miR-21. Only one well-defined band in lanes 1–4 is exhibited. Lane 4 shows a fast-migrated rate because of the low molecular weight of miR-21. The one bright band in lane 5 (without miR-21) can be observed, confirming no reaction occurred for it. In the presence of miR-21, lane 6 shows many bright bands, demonstrating the successful assembly of many H1 and H2 to form chain-like DNA polymers.

### 3.2. Electrochemical characterization of fabricated biosensor

EIS is effective for exploring GE stepwise assembly processes. An ideal Nyquist plot consists of a linear part and a hemicycle portion, corresponding to diffusion from the solution to the interface and the electron transfer-limited process. Higher-frequencies diameter refers to the electron transfer resistance ($R_{ct}$). Electron transfer kinetics processes were analyzed via the Randles equivalent circuit. Fig. 1 shows the gradual modification processes of the biosensor; curve a shows the smallest hemicycle of the bare GE, suggesting the fast charge transfer on the GE surface. The

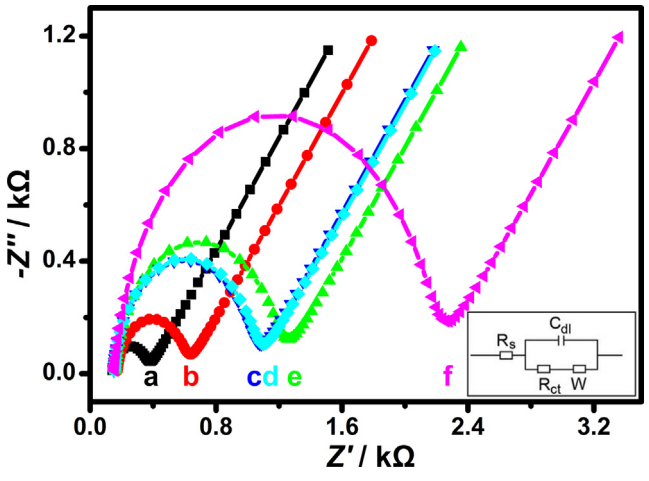


**Fig. 1.** Nyquist plots of stepwise assembly possess: (a) bare GE, (b) cDNA/GE, (c) cDNA/MCH/GE, (d) cDNA/MCH/H1/H2/GE, (e) cDNA/MCH/miR-21/GE, and (f) cDNA/MCH/H1/H2/miR-21/GE. The detection was analyzed in 5.0 mM of $[Fe(CN)_6]^{3-/4-}$ containing 0.1 M of KCl (0.1 Hz–100 kHz); Open current potential: 0.24 V, amplitude: 0.01, n = 10.

smallest $R_{ct}$ (257 Ω) is also obtained through the Randles equivalent circuit. After introducing cDNA onto the bare GE surface, the $R_{ct}$ (433 Ω) consequently increases, which is attributed to the steric hindrance formed by the self-assembly of cDNA (curve b). Increased $R_{ct}$ also suggests the successful assembly between cDNA and bare GE. After MCH was modified on the electrode surface, the $R_{ct}$ (882 Ω) further increased (curve c), which is due to the MCH film blocking the unreaction sites. Subsequently, the $R_{ct}$ (1040 Ω) increases further when the target miR-21 was incubated on the modified GE (curve e). Curve d (R = 895 Ω) exhibits a semicircle diameter similar to that of curve c, demonstrating that the HCR process cannot be triggered without miR-21. The cDNA/MCH/H1/H2/miR-21/GE (curve f) exhibits the largest $R_{ct}$ (2230 Ω). The remarkable semicircle increase of the cDNA/MCH/H1/H2/miR-21/GE suggests a successful and acceptable GE hybridization strategy process. Fig. S2 shows the data of the red curve and the black curve are consistent, demonstrating that the equivalent circuit is justified for explaining the proposed sensors.

To achieve the best analytical performance of this proposed strategy, investigating some potentially effects is necessary. Different concentrations ranging from 0.5 to 10 μM of cDNA immobilized on the GE were optimized (Fig. 2A). The $R_{ct}$ value originally increased with an increase of the cDNA concentration, then it become stable from 5 μM to 10 μM. Therefore, 5 μM was selected as the best cDNA concentration. Fig. 2B shows a similar trend, illustrating that the best H1 and H2 incubation concentration was 2.5 μM. Simultaneously, the effect of the hybridization time of cDNA was investigated, ranging from 10 h to 18 h (Fig. 2C). Results show that the maximum $R_{ct}$ value was obtained at 14 h. Also, the maximum $R_{ct}$ value was generated when the miR-21 hybridization time reached 60 min (Fig. 2D), demonstrating that this is the optimal miR-21 hybridization time in this system. Moreover, the effect of the H1 and H2 incubation time was explored (Fig. 2E). Consequently, 90 min was selected as the incubation time for whole experiments.

EIS spectra were utilized to assess the sensitivity, linear range, and limit of detection (LOD) of the proposed biosensor. Fig. 3A shows that the $R_{ct}$ value gradually increased as the miR-21concentration increased. Fig. 3B shows that the calibration plots EIS response exhibited a good linear range from 10 fM to 50 pM; the linear equation is $\Delta R_{ct} = -0.01907 + 0.35955 \log C_{miR\text{-}21}$ (pM) (R = 0.9988). The LOD is evaluated as 4.63 fM (S/N = 3), which is competitive with the values in previous reports (Table 2). Moreover, the EIS can be a label-free electrochemical method, achieving transduction in the absence of labeled species. This label-free electrochemical method also shortens biosensor preparation time. In some typical labeled electrochemical biosensors, various nanoparticles with electrocatalytic properties, such as Au nanoparticles, metallic oxide, and metal sulfide, should be prepared first, thereby expanding the time detection. Therefore, the proposed electrochemical impedimetric biosensor provided a novel method for detecting other biomarkers.

To validate the established biosensor accuracy, an examination was conducted of the miR-21 in 10% human serum. Real samples were spiked with certain amounts of miR-21 to detect and calculate recoveries. Table 3 shows that miR-21 recoveries range from 83.61% to 118.61% with RSD ranging from 0.96% to 9.67%, suggesting the proposed sensor accuracy was desirable.

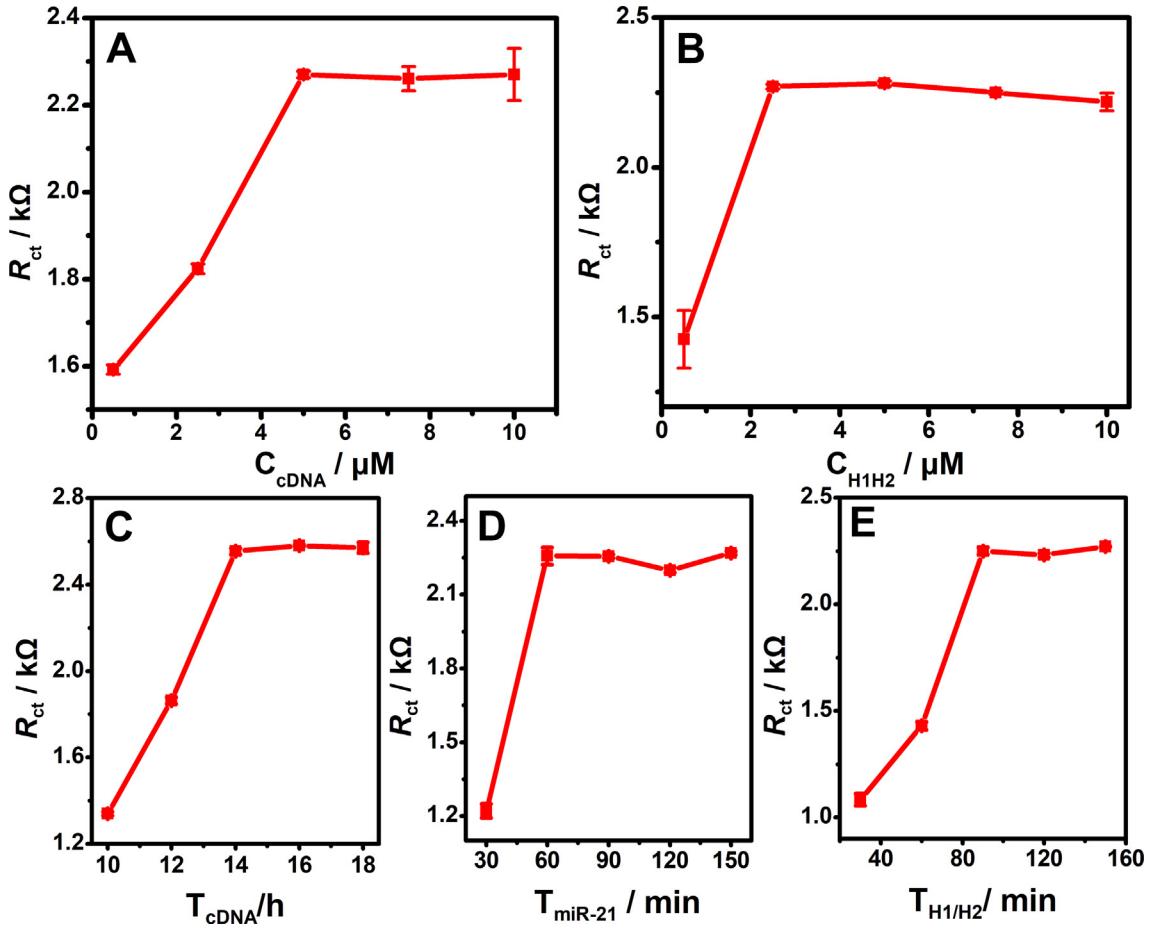


**Fig. 2.** Influence of the cDNA (A) and H1, H2 (B) concentrations. Effects of hybridization time of cDNA (C), miR-21 (D) and H1, H2 (E), n = 10.

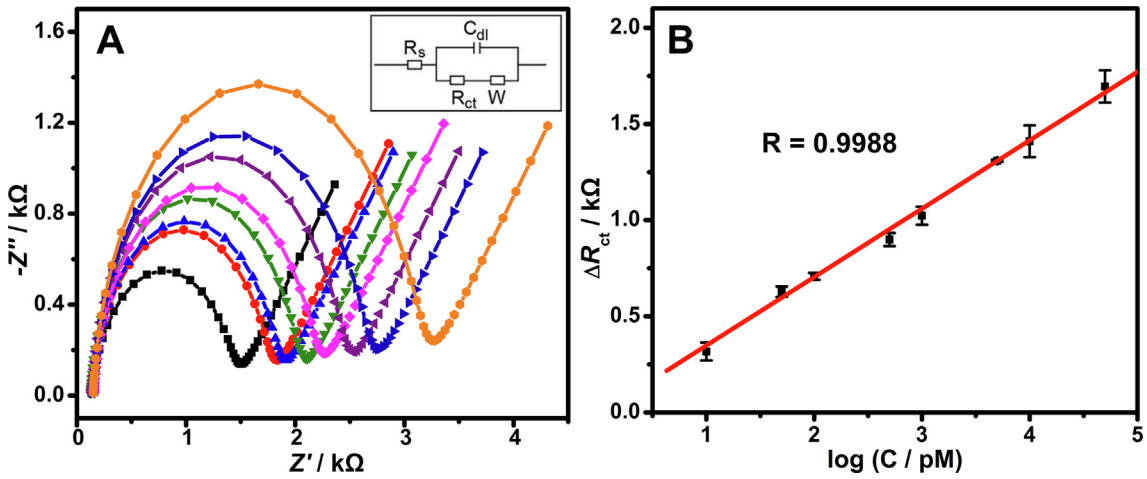


**Fig. 3.** EIS responses of the fabricated biosensor with different concentrations of miR-21(10 fM to 50 pM) (A); The detection was analyzed in 5.0 mM of $[Fe(CN)_6]^{3-/4-}$ containing 0.1 M of KCl (0.1 Hz–100 kHz); Open current potential: 0.24 V, amplitude: 0.01. Calibration plot of the $\Delta R_{ct}$ vs. the logarithm of miR-21 concentration (B), n = 10.

**Table 2**
Comparison of different methods for detection of miRNA.

| Materials | Analytical technique | Linear range | Limit of detection | Reference |
|---|---|---|---|---|
| biotin-MB-AuNPs[a] | EIS | 1–1000 pM | 300 fM | [27] |
| CdTe nanocrystals and Au nanoclusters[b] | ECL[c] | 100 fM–100 nM | 21.7 fM | [38] |
| Electrode-free | Colorimetric | 0–0.1 nM | 32 fM | [39] |
| ss-DNA/MWCNT/MB/GCE[d] | DPV[e] | 0.1–500 pM | 84.3 fM | [40] |
| Au@NP$Fe_2O_3$NC[f] | DPV | 500 fM–5 nM | 100 fM | [41] |
| Arched Probe Mediated Isothermal Exponential Amplification | DPV | 20 fM–10 nM | 5.36 fM | [42] |
| MBA-AuNPs/DA-AuNPs[g] | DPV | 100 fM–10 pM | 45 fM | [43] |
| Hairpin capture probe/target recycling/MB[h] | DPV | 0.5 pM–2 nM | 56 fM | [44] |
| $MoS_2$-Thionine-AuNPs[i] | SWV[j] | 1 pM–10 nM | 260 fM | [45] |
| GO-CA-PGEs[k] | EIS | 355–2130 nM | 41.2 nM | [46] |
| Dendrimer-SPE[l] | EIS | 140–360 nM | 74 nM | [47] |
| polypyrrole | EIS | 5–80 pM | 2 pM | [48] |
| **cDNA/MCH/H1/H2/miR-21/GE** | **EIS** | **10 fM–50 pM** | **4.63 fM** | **This work** |

[a] Molecular beacon probe was conjugated with gold nanoparticles.
[b] CdTe nanocrystals and Au nanoclusters modified on glassy carbon electrode (GCE).
[c] Electrochemiluminescence.
[d] miRNA/single strands DNA (ss-DNA)/multi-walled carbon nanotube/molecular blue modified on GCE.
[e] Differential pulse voltammetry.
[f] Gold-loaded nanoporous iron oxide nanocubes.
[g] 4-mercaptophenylboronic acid -capped gold nanoparticles /dopamine -capped gold nanoparticles.
[h] Hairpin capture probe/target recycling/methyl blue.
[i] Thionine and gold nanoparticles co-functionalized $MoS_2$ nanosheet.
[j] Square wave voltammetry.
[k] Graphene oxide/covalent agents/pencil graphite electrodes.
[l] Poly(amidoamine) dendrimer modified single-use screen printed carbon electrode.

**Table 3**
The proposed biosensor applied in 3 human serum samples.

| Human serums | Added (fM) | Founded (fM) | Recovery (%) | RSD (%) |
|---|---|---|---|---|
| 1 | 0 | 1.3 | – | 0.96 |
| | 100 | 119.9 | 118.61 | 1.60 |
| | 500 | 419.35 | 83.61 | 1.40 |
| 2 | 0 | 0.63 | – | 9.10 |
| | 100 | 108.64 | 108 | 3.47 |
| | 500 | 492.31 | 98.34 | 9.67 |
| 3 | 0 | 0.15 | – | 3.00 |
| | 100 | 112.47 | 112.33 | 1.16 |
| | 500 | 488.53 | 97.68 | 1.70 |

To investigate the selectivity of this proposed method, miR-199a, miR-155, and miR-144 sequences replaced the target miR-21(Fig. 4A). A lower $\Delta R_{ct}$ value of miR-199a, miR-155, and miR-144 sequences was noticed when compared to the $\Delta R_{ct}$ of the target miR-21. Moreover, the biosensor incubated with the mixed samples exhibited a similar $\Delta R_{ct}$ value when only miR-21 was present. These results show that the proposed electrochemical impedimetric biosensor is efficiently selective toward miR-21.

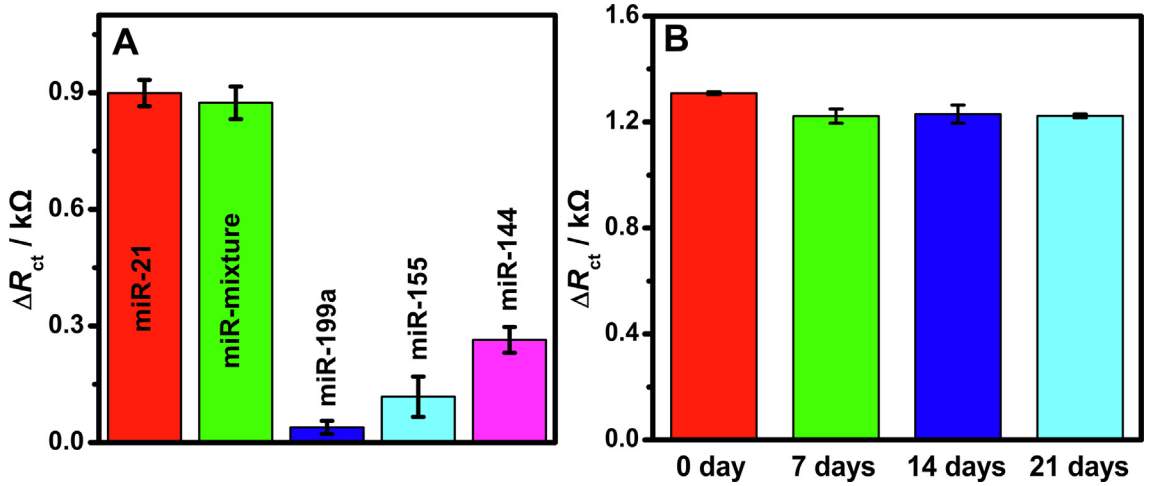


**Fig. 4.** EIS responses of the proposed biosensor for the detection of different miRNA sequences, including $5.0 \times 10^{-7}$ μM of miR-21, $5.0 \times 10^{-6}$ μM of miR-199a, $5.0 \times 10^{-6}$ μM of miR-155, $5.0 \times 10^{-6}$ μM of miR-144, and the mixture of the four kinds of miRNAs (A). The storage stability of the miR-21 biosensor at 4 °C (B), n = 10.

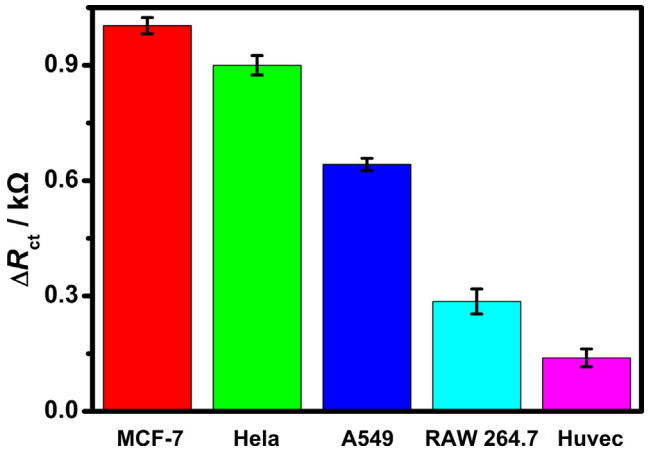


**Fig. 5.** EIS responses for detecting miR-21 produced from MCF-7, HeLa, A549, RAW 264.7, and HUVEC cells, n = 10.

To demonstrate the biosensor stability, EIS was employed to assess the self-assembly electrode change in the presence of $5.0 \times 10^{-6}$ μM of miR-21 (Fig. 4B). The prepared sensing electrodes were kept at 4 °C for different times (0, 7, 14, and 21 days). As expected, biosensor $\Delta R_{ct}$ values stored for 7, 14, and 21 days decrease less than the initial response $\Delta R_{ct}$ value. This shows that the proposed impedimetric biosensor possesses satisfactory storage stability.

Further analysis was conducted on the feasibility of the impedimetric biosensor, which was utilized to determine the content of miR-21 derived from five different cancer cells (Fig. 5). A more significant EIS response was obtained from MCF-7, HeLa, and A549 cells than that obtained from the endogenous reference genes RAW 264.7 and HUVEC. This proves the over-expression of miR-21 in HeLa, MCF-7, and A549, which conforms to the reported work [46–50].

## 4. Conclusion

In conclusion, a facile electrochemical biosensor combining efficient HCR strategy and EIS method was first clarified for sensitive miR-21 determination. The interfacial charge transfer resistance ($R_{ct}$) difference was probed via EIS and Randles equivalent circuit. HCR relies on DNA strand substitution to form alternate nucleic acid concatamers and avoid some fussy steps of protein enzymes. After amplifying via HCR, oligonucleotides with negatively charged repelling $[Fe(CN)_6]^{3-/4-}$ ions can form spatial blockages. Many linear DNA concatamers can lead to a great increase in interfacial $R_{ct}$. $R_{ct}$ positively correlated with miR-21 content enables direct and quantitative miR-21 detection. Then, the designed biochemical self-assembly strategy of this impedimetric biosensor is successfully applied to the analysis of the miR-21 expression level extracted from five different cells. This electrochemical biosensor design would help rapidly and simply detect miR-21, thereby developing a powerful clinical analysis platform.

## CRediT authorship contribution statement

**Tianjiao Meng:** Methodology, Software, Writing - original draft. **Dan Zhao:** Writing - review & editing. **Huimin Ye:** Data curation, Writing - original draft. **Yue Feng:** Methodology, Data curation. **Huan Wang:** Writing - review & editing, Funding acquisition. **Yufan Zhang:** Investigation, Methodology, Data curation, Software, Supervision, Funding acquisition.

## Declaration of Competing Interest

The authors declare that they have no known competing financial interests or personal relationships that could have appeared to influence the work reported in this paper.

## Acknowledgements

The authors gratefully acknowledge the support from the Priority Strategy Project of Key Laboratory of Medicinal Chemistry and Molecular Diagnosis of Ministry of Education (No. ts2019003), the Natural Science Foundation of Hebei Province (No. B2019201407 and No. B2018201214), the Science and Technology Research Project of Higher Education Institutions in Hebei Province (QN2020153), the Advanced Talents Incubation Program of the Hebei University (No.801260201026), and the Laboratory Opening Program of the Hebei University (No. sy201831).

## Appendix A. Supplementary data

Supplementary data to this article can be found online at https://doi.org/10.1016/j.jcis.2020.05.118.

## References


[1] L. Wang, T. Meng, D. Zhao, H. Jia, S. An, X. Yang, et al., An enzyme-free electrochemical biosensor based on well monodisperse Au nanorods for ultrasensitive detection of telomerase activity, Biosens. Bioelectron. 148 (2020) 111834.

[2] T. Meng, H. Jia, H. Ye, T. Zeng, X. Yang, H. Wang, et al., Facile preparation of $CoMoO_4$ nanorods at macroporous carbon hybrid electrocatalyst for non-enzymatic glucose detection, J. Colloid Interface Sci. 560 (2020) 1–10.

[3] L. Wang, T. Meng, G. Yu, S. Wu, J. Sun, H. Jia, et al., A label-free electrochemical biosensor for ultra-sensitively detecting telomerase activity based on the enhanced catalytic currents of acetaminophen catalyzed by Au nanorods, Biosens. Bioelectron. 124–125 (2019) 53–58.

[4] L. Wang, T. Meng, L. Liang, J. Sun, S. Wu, H. Wang, et al., Fabrication of amine-functionalized metal-organic frameworks with embedded palladium nanoparticles for highly sensitive electrochemical detection of telomerase activity, Sens. Actuators B 278 (2019) 133–139.

[5] H. Cheng, W. Li, S. Duan, J. Peng, J. Liu, W. Ma, et al., Mesoporous silica containers and programmed catalytic hairpin assembly/hybridization chain reaction based electrochemical sensing platform for miRNA ultrasensitive detection with low background, Anal. Chem. 16 (2019) 10672–10678.

[6] J. Wang, J. Lu, S. Dong, N. Zhu, E. Gyimah, K. Wang, et al., An ultrasensitive electrochemical biosensor for detection of microRNA-21 based on redox reaction of ascorbic acid/iodine and duplex-specific nuclease assisted target recycling, Biosens. Bioelectron. 130 (2019) 81–87.

[7] K. An, X. Lu, C. Wang, J. Qian, Q. Chen, N. Hao, et al., Porous gold nanocages: high atom utilization for thiolated aptamer immobilization to well balance the simplicity, sensitivity, and cost of disposable aptasensors, Anal. Chem. 91 (2019) 8660–8666.

[8] N. Formisano, P. Jolly, N. Bhalla, M. Cromhout, S.P. Flanagan, R. Fogel, et al., Optimisation of an electrochemical impedance spectroscopy aptasensor by exploiting quartz crystal microbalance with dissipation signals, Sens. Actuators B 220 (2015) 369–375.

[9] D. Ortizaguayo, M.D. Valle, Label-free aptasensor for lysozyme detection using electrochemical impedance spectroscopy, Sensors 18 (2018) 354–365.

[10] C. Gulsah, E. Arzum, PAMAM dendrimer modified screen printed electrodes for impedimetric detection of miRNA-34a, Microchem. J. 148 (2019) 748–758.

[11] R. Miranda-Castro, R. Sanchez-Salcedo, B. Suarez-Alvarez, N. de-los-Santos-Alvarez, A.J. Miranda-Ordieres, M. Jesus Lobo-Castanon, Thioaromatic DNA monolayers for target-amplification-free electrochemical sensing of environmental pathogenic bacteria, Biosens. Bioelectron. 92 (2017) 162–170.

[12] S. Azzouzi, W.C. Mak, K. Kor, A.P. Turner, M.B. Ali, V. Beni, An integrated dual functional recognition/amplification bio-label for the one-step impedimetric detection of micro-RNA-21, Biosens. Bioelectron. 92 (2017) 154–161.

[13] P. Kannan, P. Subramanian, T. Maiyalagan, Z. Jiang, Cobalt oxide porous nanocubes-based electrochemical immunobiosensing of hepatitis B virus DNA in blood serum and urine samples, Anal. Chem. 91 (2019) 5824–5833.

[14] B. Wightman, I. Ha, G. Ruvkun, Posttranscriptional regulation of the heterochronic gene lin-14 by lin-4 mediates temporal pattern formation in C. elegans, Cell 75 (1993) 855–862.

[15] S. Jonas, E. Izaurralde, Towards a molecular understanding of microRNA-mediated gene silencing, Nat. Rev. Genet. 16 (2015) 421–433.

[16] F. Yang, Y. Cheng, Y. Cao, Y. Zhang, H. Dong, H. Lu, et al., MicroRNA triggered DNA "Nano Wheel" for visualizing intracellular microRNA via localized DNA cascade reaction, Anal. Chem. 91 (2019) 9828–9835.

[17] Z. Su, Z. Yang, Y. Xu, Y. Chen, Q. Yu, MicroRNAs in apoptosis autophagy and necroptosis, Oncotarget 6 (2015) 8474–8490.

[18] J. Zhang, M. He, C. Nie, M. He, Q. Pan, C. Liu, et al., Biomineralized metal-organic framework nanoparticles enable enzymatic rolling circle amplification in living cells for ultrasensitive microRNA imaging, Anal. Chem. 91 (2019) 9049–9057.

[19] H. Tang, J. Zhu, D. Wang, Y. Li, Dual-signal amplification strategy for miRNA sensing with high sensitivity and selectivity by use of single Au nanowire electrodes, Biosens. Bioelectron. 131 (2019) 88–94.

[20] V. Kakkassery, R. Schroers, S.E. Coupland, M.I. Wunderlich, M. Schargus, C. Heinz, et al., Vitreous microRNA levels as diagnostic biomarkers for vitreoretinal lymphoma, Blood 129 (2017) 3130–3133.

[21] Y. Pang, C. Wang, L. Lu, C. Wang, Z. Sun, R. Xiao, Dual-SERS biosensor for one-step detection of microRNAs in exosome and residual plasma of blood samples for diagnosing pancreatic cancer, Biosens. Bioelectron. 130 (2019) 204–213.

[22] Q. Wu, H. Wang, K. Gong, J. Shang, X. Liu, F. Wang, Construction of an autonomous nonlinear hybridization chain reaction for extracellular vesicles-associated microRNAs discrimination, Anal. Chem. 91 (2019) 10172–10179.

[23] J. Lu, J. Wang, X. Hu, E. Gyimah, S. Yakubu, K. Wang, et al., Electrochemical biosensor based on tetrahedral DNA nanostructures and G-Quadruplex-hemin conformation for the ultrasensitive detection of microRNA-21 in serum, Anal. Chem. 91 (2019) 7353–7359.

[24] M. Li, W. Zhao, H. Wang, X. Li, C. Xu, H. Chen, et al., Dynamic single molecular rulers: toward quantitative detection of microRNA-21 in living cells, Anal. Chem. 90 (2018) 14255–14259.

[25] X. Liu, S. Zhang, Z. Cheng, X. Wei, T. Yang, Y. Yu, et al., Highly sensitive detection of microRNA-21 with ICPMS via hybridization accumulation of upconversion nanoparticles, Anal. Chem. 90 (2018) 12116–12122.

[26] O. Salamin, T. Kuuranne, M. Saugy, N. Leuenberger, Loop-mediated isothermal amplification (LAMP) as an alternative to PCR: a rapid on-site detection of gene doping, Drug Test. Anal. 9 (2017) 1731–1737.

[27] D. Li, W. Cheng, Y. Li, Y. Xu, X. Li, Y. Yin, et al., Catalytic hairpin assembly actuated DNA nanotweezer for logic gate building and sensitive enzyme-free biosensing of microRNAs, Anal. Chem. 88 (2016) 7500–7506.

[28] S. Tang, Y. Gu, H. Lu, H. Dong, K. Zhang, W. Dai, et al., Highly-sensitive microRNA detection based on bio-bar-code assay and catalytic hairpin assembly two-stage amplification, Anal. Chim. Acta 1004 (2018) 1–9.

[29] Z. Chen, Y. Liu, C. Xin, J. Zhao, S. Liu, A cascade autocatalytic strand displacement amplification and hybridization chain reaction event for label-free and ultrasensitive electrochemical nucleic acid biosensing, Biosens. Bioelectron. 113 (2018) 1–8.

[30] T. Kilic, A. Erdem, M. Ozsoz, S. Carrara, MicroRNA biosensors: opportunities and challenges among conventional and commercially available techniques, Biosen. Bioelectron. 99 (2017) 525–546.

[31] S. Liu, L. Fang, Y. Wang, L. Wang, Universal dynamic DNA assembly-programmed surface hybridization effect for single-step, reusable, and amplified electrochemical nucleic acid biosensing, Anal. Chem. 89 (2017) 3108–3115.

[32] Y. Liu, H. Wang, C. Xiong, Y. Chai, R. Yuan, An ultrasensitive electrochemiluminescence immunosensor for NT-proBNP based on self-catalyzed luminescence emitter coupled with PdCu@carbon nanohorn hybrid, Biosens. Bioelectron. 87 (2017) 779–785.

[33] Y. Tang, X. Zhang, L. Tang, R. Yu, J. Jiang, In situ imaging of individual mRNA mutation in single cells using ligation-mediated branched hybridization chain reaction (ligation-bHCR), Anal. Chem. 89 (2017) 3445–3451.

[34] F. Yin, H. Liu, Q. Li, X. Gao, Y. Yin, D. Liu, Trace microRNA quantification by means of plasmon-enhanced hybridization chain reaction, Anal. Chem. 88 (2016) 4600–4604.

[35] L. Zhou, Y. Wang, C. Yang, H. Xu, J. Luo, W. Zhang, et al., A label-free electrochemical biosensor for microRNAs detection based on DNA nanomaterial by coupling with Y-shaped DNA structure and non-linear hybridization chain reaction, Biosens. Bioelectron. 126 (2019) 657–663.

[36] F. Zhang, S. Wang, J. Feng, R. Zou, L. Xiang, C. Cai, $MoS_2$-loaded G-quadruplex molecular beacon probes for versatile detection of microRNA through hybridization chain reaction signal amplification, Talanta 202 (2019) 342–348.

[37] Y. Li, C.Z. Huang, Y.F. Li, Ultrasensitive electrochemiluminescence detection of microRNA via one-step introduction of a target-triggered branched hybridization chain reaction circuit, Anal. Chem. 91 (2019) 9308–9314.

[38] M.M. Kamal, M.N. Islam, M.H. Haque, S. Tanaka, V. Gopalan, G. Alici, et al., Gold-loaded nanoporous superparamagnetic nanocubes for catalytic signal amplification in detecting miRNA, Chem. Commun. 53 (2017) 8231–8234.

[39] Y. Yu, Z. Chen, L. Shi, F. Yang, J. Pan, B. Zhang, et al., Ultrasensitive electrochemical detection of microRNA based on an arched probe mediated isothermal exponential amplification, Anal. Chem. 86 (2014) 8200–8205.

[40] N. Xia, L. Zhang, G. Wang, Q. Feng, L. Liu, Label-free and sensitive strategy for microRNAs detection based on the formation of boronate ester bonds and the dual-amplification of gold nanoparticles, Biosen. Bioelectron. 47 (2013) 461–466.

[41] L. Zhou, W. Jian, Z. Chen, J. Li, T. Wang, Z. Zhang, et al., A universal electrochemical biosensor for the highly sensitive determination of microRNAs based on isothermal target recycling amplification and a DNA signal transducer triggered reaction, Microchim. Acta 184 (2017) 1305–1313.

[42] D. Zhu, W. Liu, D. Zhao, Q. Hao, J. Li, J. Huang, et al., Label-free electrochemical sensing platform for microRNA-21 detection using thionine and gold nanoparticles Co-functionalized $MoS_2$ nanosheet, ACS Appl. Mater. Interfaces 9 (2017) 35597–35603.

[43] A. Erdem, E. Eksin, D. Isin, D. Polat, Graphene oxide modified chemically activated graphite electrodes for detection of microRNA, Electroanalysis 29 (2017) 1350–1358.

[44] G. Congur, E. Eksin, A. Erdem, Multi channel screen printed array of electrodes for enzyme-linked voltammetric detection of microRNAs, Sens. Actuators A 279 (2017) 493–500.

[45] J. Mandli, A. Amine, Efficient oxidation of hydrazine using amine-functionalized cobalt and nickel porphyrin-modified electrodes, J. Solid State Electrochem. 22 (2018) 1007–1014.

[46] H. Cheng, J. Liu, W. Ma, S. Duan, J. Huang, X. He, et al., Low background cascade signal amplification electrochemical sensing platform for tumor-related mRNA quantification by target-activated hybridization chain reaction and electroactive cargo release, Anal. Chem. 90 (2018) 12544–12552.

[47] Y. Zhang, Z. Yue, P. Wang, Y. Li, J. Xin, M. Pang, et al., Cisplatin upregulates $MSH_2$ expression by reducing miR-21 to inhibit A549 cell growth, Biomed. Pharmacother. 67 (2013) 97–102.

[48] A. Subedi, J.K. Mi, S. Nepal, E.S. Lee, J.A. Kim, D.H. Sohn, et al., Globular adiponectin modulates expression of programmed cell death 4 and miR-21 in RAW 264.7 macrophages through the MAPK/NF-κB pathway, FEBS Lett. 587 (2013) 1556–1561.

[49] Y. Liu, F. Luo, B. Wang, H. Li, Y. Xu, X. Liu, et al., STAT3-regulated exosomal miR-21 promotes angiogenesis and is involved in neoplastic processes of transformed human bronchial epithelial cells, Cancer Lett. 370 (2016) 125–135.

[50] M. Sun, J. Liu, Y. Chai, J. Zhang, Y. Tang, R. Yuan, Three-dimensional cadmium telluride quantum dots–DNA nanoreticulation as a highly efficient electrochemiluminescent emitter for ultrasensitive detection of microRNA from cancer cells, Anal. Chem. 91 (2019) 7765–7773.